



POLITECNICO
MILANO 1863

DIPARTIMENTO DI MECCANICA

mecc



Focusing tube operational vibration as a means for monitoring the abrasive waterjet cutting capability

Copertaro, E.; Perotti, F.; Castellini, P.; Chiariotti, P.; Martarelli, M.; Annoni, M.

This is a post-peer-review, pre-copyedit version of an article published in JOURNAL OF MANUFACTURING PROCESSES. The final authenticated version is available online at: <http://dx.doi.org/10.1016/j.jmapro.2020.09.040>

This content is provided under [CC BY-NC-ND 4.0](https://creativecommons.org/licenses/by-nc-nd/4.0/) license



Focusing tube operational vibration as a means for monitoring the abrasive waterjet cutting capability

Edoardo Copertaro ^(a), Francesco Perotti ^(b), Paolo Castellini ^(c), Paolo Chiariotti ^(c), Milena Martarelli ^(c)
Massimiliano Annoni ^(b)

- (a) *Université du Luxembourg, Faculté des Sciences, de la Technologie et de la Communication, Avenue de l'Université, L-4365, Esch-sur-Alzette, Luxembourg*
- (b) *Politecnico di Milano, Dipartimento di Meccanica, Via Privata Giuseppe La Masa 1, 20156, Milano, Italia*
- (c) *Università Politecnica delle Marche, Dipartimento di Ingegneria Industriale e Scienze Matematiche, Via Brecce Bianche 12, 60131, Ancona, Italia*

Corresponding author Edoardo Copertaro

Contact details

Postal address:	12, Rue Ancienne Cote d'Eich, 1459, Luxembourg Ville (L)
Email:	edoardo.copertaro@uni.lu
Office:	+ 352 466 644 6836
Fax:	+ 352 466 644 35790
Mobile 1:	+ 39 338 658 1667
Mobile 2:	+ 352 661 369 501

Abstract

Abrasive waterjet cutting is a competitive manufacturing technology in the aerospace, defense and automotive industries which, as power users, require state of the art process performances in terms of stability and product assurance, due to their demanding quality standards. Meeting such requirements is a relevant technical challenge for abrasive waterjet cutting, due to insufficient monitored data and intrinsic process instability. The present paper describes an innovative approach based on non-invasive vibration sensors, for monitoring the jet cutting capability. This result is allowed by the experimental evidence proving that the operational vibration monitored by means of two accelerometers installed at the tip of the focusing tube is well related to the kinetic power of the abrasive particles, i.e. the only portion of the jet power that is responsible for the material removal in abrasive waterjet cutting. The approach is validated by means of an experimental investigation, in which the abrasive waterjet is fired at different water pressures and abrasive mass flow rates, providing different kinetic powers. The information delivered enriches the process knowledge, thus paving the way to significant improvements ranging from closed-loop control strategies for the water and abrasive feeding systems to actions for supporting operators in compensating drifts of the jet cutting capability. The expected impact is an improvement of process automation and stability, as well as an enhanced process traceability.

Keywords

Abrasive Waterjet Cutting; Vibration Measurements; Process Monitoring.

Nomenclature of the abrasive waterjet cutting technology

Letters / Greek letters	
p	Water pressure
m_a	Abrasive mass flow rate
v_{th}	Theoretical velocity (Bernoulli)
ρ	Water density
$v_{th,c}$	Theoretical compressible velocity
C, L	Constants
v_j	Real jet velocity (or pure waterjet velocity)
c_v	Velocity coefficient
ψ	Compressibility coefficient
m_w	Water mass flow rate
Q_w	Water volume flow rate
S_j	Jet cross-sectional area at the <i>vena contracta</i>
c_c	Contraction coefficient
d_n	Orifice diameter
S_0	Nominal cross-sectional area of the orifice
c_d	Discharge coefficient
r_d	Abrasive loading ratio
v_{abr}	Abrasive waterjet velocity
P_{part}	Kinetic power of the abrasive particles (for the sake of brevity jet power)
$P_{part,spec}$	Specific kinetic power of the abrasive particles (for the sake of brevity jet specific power)
d_{awj}	Focusing tube diameter
Subscripts	
0	Upstream section
1	Downstream section

1 Introduction

Abrasive Waterjet Cutting (AWJC) is a very competitive technology in the aerospace, defense, and automotive industries. Here the competitive edge with respect to other technologies is due to the lower initial investment and the absence of a heat-affected zone on the workpiece. Other advantages include: no limitations in shape complexity; no mechanical contact with physical tools, which makes it very delicate on fragile and/or composite materials; narrow kerf, down to 0.3 mm; negligible blurs; good edge sharpness [1]. However, said reference industrial sectors require enhanced process performances in terms of stability and product quality assurance, due to their tight safety and quality standards. Meeting such requirements is a relevant technical challenge for AWJC, because of insufficient monitoring and control capabilities of standard machines [2]. The tracking and stabilization of the AWJC process constitutes the motivation of this contribution. In particular, the present research lies in the field of vibroacoustic process monitoring, which is widely documented in literature as an interesting means for extracting relevant AWJC process information that could be beneficial for the purpose.

The terminal part of the AWJC apparatus, i.e. the cutting head, is depicted in Figure 1: here water flows through the primary orifice at very high pressure (up to 600 MPa) resulting in a high-speed (about 1000 m/s) waterjet; abrasive particles are fed with air into the mixing chamber; the resulting abrasive jet travels through the focusing tube and momentum is transferred to the particles, which are consequently accelerated; finally, the abrasive jet exits the focusing tube, gets airborne, then impinges on the workpiece producing the removal of material [3]. In an AWJC apparatus, the main controlled parameters are the following: water pressure (p); traverse speed (or feed rate); abrasive mass flow rate (m_a); standoff distance, i.e. the distance between the tip of the focusing tube and the workpiece. It is common practice to maintain the standoff distance between 1 and 2 mm, which is widely accepted as the optimal value for most of the scenarios. Cutting performance models are used by the waterjet machine tool builders in their Computer Numerical Control (CNC) software for selecting p , m_a and the traverse speed: the latter is usually set at the highest value that is allowed by the target quality of the kerf walls and edges (basically the surface roughness and the kerf taper), whilst p and m_a are typically set at the highest values that are allowed by the equipment. Said selection strategy of the process parameters is effective in improving productivity. The water pressure is obtained and controlled by an intensifier or direct drive pump and typically ranges between 300 and 400 MPa, even if pumps up to 600 MPa exist on the market. The abrasive mass flow rate is controlled by means of different kinds of feeders (belt-based, screw-based and others) and ranges between 100 and 400 g/min, apart from high precision cutting, where it can go down to 3-5 g/min [4].

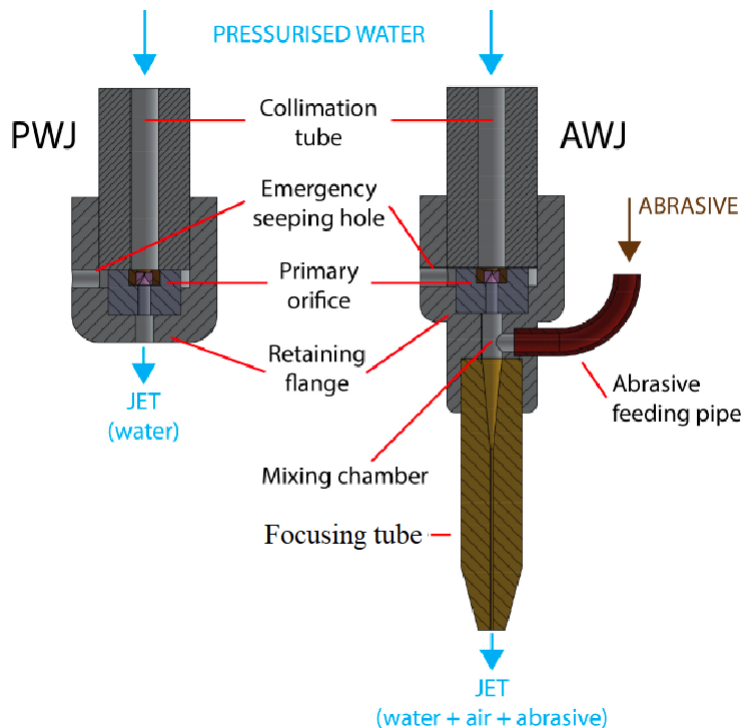


Figure 1 AWJC head (PWJ: pure waterjet; AWJ: abrasive waterjet) [4].

The jet cutting capability is possibly the most important AWJC performance indicator, which is controlled by the two operated parameters p and m_a and correlates very closely with the final quality of the workpiece, as well as productivity. For such reason, both the absolute value and stabilization of the jet cutting capability are of great concern for the waterjet machine tool builders. This is particularly true for critical applications that require very

high accuracy and absolute integrity of the cutting edge, e.g. no cracks on fragile materials. Indeed, further process variables besides p and m_a concur to the fluctuation and drift versus time of the jet cutting capability, the most relevant are the instantaneous quantity of abrasive particles inside the mixing chamber and the focusing tube inner diameter: the first can suddenly reduce with detrimental effects on the cutting performance [5]; the second tends to increase due to the wear progression of the focusing tube [6]. It is evident that any effort towards the stabilization of the jet cutting capability must rely on its effective monitoring. Indeed, having such an in-line information available would enable the implementation of closed-loop controls of p and m_a , which are expected to be more effective for the purpose, with respect to the open loops currently in use. Unfortunately, the current AWJC systems do not carry sensors that can deliver such information, being the monitored variables mostly limited to pressure, temperature, position, displacement and power absorptions [7]. This paper aims at demonstrating how vibroacoustic sensors are the right choice for monitoring the AWJC capability. Indeed, vibroacoustic sensors have extensively proven their capability of delivering robust estimators of specific target variables; besides, the installation of these sensors is generally non-invasive and compatible with the underlying hardware.

The vibration and acoustic emissions have been used by different researchers for the in-line monitoring of AWJC processes. The literature review has shown that a first category of methods deals with the monitoring of process and workpiece parameters, including the final quality. A second category is related to the diagnostics and condition monitoring of machine components. Regarding the first category, most of the experimental investigations rely on the extraction of synthetic indicators, e.g. the Root Mean Square (RMS) of a monitored signal, which were proven to be sensitive to the target parameters.

Hassan et al. [8] investigated the acoustic emission during the AWJC of AISI 1018 carbon steel workpieces, with the scope of monitoring the actual cutting depth. The measurement set-up included two acoustic sensors that were attached to the edge of the workpiece, nearby the cutting path. The authors found that the RMSs of the acoustic signals were linearly proportional to the cut depth, hence can be effectively used as indicators of this important process parameter.

Jurisevic et al. [9] explored the relationship existing between the standoff distance and the acoustic emission during AWJC experiments carried out on aluminium alloy sheets, while the other process parameters were maintained constant. Two synthetic indicators were defined, namely the RMS of the acoustic signal and the amplitude cumulative sum of its power spectrum. Both the indicators showed a linear correlation with the standoff distance for limited thicknesses of the workpiece, hence can be exploited for the purpose of its monitoring in real time.

In [10], the authors proved the possibility of using the level of acoustic pressure to predict the transverse speed, therefore the surface roughness in AWJC. The acoustic pressure was measured by means of a modular sound analyser, which was installed nearby the cutting head. Indeed, the relationship between the level of acoustic pressure and the transverse speed was proven, thus enabling the implementation of a closed loop control system for controlling and supervising the workpiece quality.

Peržel et al. [11] developed a method for monitoring in real time the technology efficiency of the material removal process. Vibration signals were measured on an AISI 309 stainless steel workpiece, during AWJC operations carried out at different m_a . The measurement setup included four uniaxial accelerometers, which were installed on the edge of the workpiece. The signals were processed in the frequency domain and correlations between the spectral amplitudes at certain frequencies and the surface topography of the workpiece, hence its quality, were proven.

The effects of m_a , the transverse speed and the focusing tube inner diameter on the emitted vibration during AWJC operations were investigated by Hreha et al. [12]. Vibration signals were gathered by means of accelerometers, which were installed on an AISI 309 stainless steel workpiece. The vibration signals were analysed both in the time and frequency domain. Finally, the sensitivities of their power spectra to said process parameters were proven.

Popan et al. [13] conducted an experimental study regarding the AWJC of Composite Fiber Reinforced Panel (CFRP) materials. Cutting experiments were carried out at different traverse speeds and the acoustic emission was monitored by means of two sensors, of which one was installed on the cutting head and the other on the workpiece. Subsequently, the correlation between the acoustic emission and the traverse speed, hence the surface roughness of the workpiece, was proven.

In [14] the authors used the vibroacoustic emission during AWJC of CFRP, titanium and CFRP-titanium stacks, for the purpose of process control. Frequency ranges were identified by analysing the monitored signals, which showed sensitivity to p and the traverse speed. Overall, the study was successful in identifying signals characteristics that can be used for process control and troubleshooting.

In [15], the acoustic emission of AWJC was used by the authors for the in-line assessment of the surface quality of the workpiece. Here cutting experiments were carried out on aluminium 5251 panels at different traverse speeds and the influence of this parameter on the surface quality was analyzed. At the same time, the acoustic emission from the workpiece was monitored by means of a structure-borne sensor and up to 1000 kHz. Subsequently, the correlation between the acoustic emission and the traverse speed, hence the surface quality, was proven.

Recently, a novel method was proposed in [16] for the monitoring of p and m_a in AWJC of titanium-CFRP stacks. In this investigation, acoustic signals were gathered and subsequently processed by means of wavelet decomposition. It was found that the time-localized feature of the wavelet filters can be well exploited for enhancing relevant characteristics of the monitored signals.

In [17], the acoustic emission during AWJ drilling of Inconel 718 and AISI 1040 steel was proposed as a tool for process monitoring. The investigation proved that the RMSs of the gathered signals were correlated to the penetration rate, as well as the type of worked material. A further conclusion concerned the possibility of using this method for identifying anomalies in the current cutting run, once a benchmark data set has been made available.

Other methods are focused on the exploitation of the AWJC vibroacoustic emission for extracting energy performance indicators of the process. The main purpose is to collect information about the input jet energy and its active fraction, i.e. the portion that is effectively used in the cutting operation and correlates closely with the penetration depth of the jet. A first attempt in this direction was made by Axinte and Kong [18]: by using a measurement setup consisting of two acoustic sensors at different locations, they proved the possibility of monitoring the active fraction of the jet energy and delivering an estimator of the penetration depth, as well as further troubleshooting information. An analogous study was proposed by Rabani et al. [19]: here the active energy was measured by means of a similar setup, and the information used as the observed variable for feeding innovative closed-loop control systems of the water pump and the abrasive feeder.

The vibroacoustic emission of an AWJC plant has been used for diagnostics and condition monitoring purposes, as well. According to Momber and Kovacevic [5], the vibroacoustic emission contains relevant information about the integrity of several components of the cutting head, in particular the primary orifice and the focusing tube. Different methods have been proposed in literature to monitor their wear progression, which rely on the correlation of the vibroacoustic emission with their geometrical features and their variations versus time.

The feasibility of using the acoustic emission as a monitoring tool for the focusing tube wear detection was investigated by Kovacevic et al. [20][21][22]. The authors analysed the power spectra of the acoustic signals that were emitted during AWJC operations. By comparing the spectra gathered with new and worn focusing tubes, a frequency range was identified at about 20 kHz, whose amplitude showed a detectable sensitivity to the wear status of the focusing tube.

A different method for monitoring the wear progression of the focusing tube was proposed by Hreha et al. [23]. Here the authors studied the vibration emitted by an AISI 309 stainless steel workpiece during AWJC operations. The monitoring setup was the same used in [12] and consisted of accelerometers installed on the workpiece. The analysis of the vibration signals showed the presence of characteristic peaks in their spectra, which were proven to be sensitive to both the inner diameter of the focusing tube and m_a . Indeed, changes of these two parameters resulted in frequency and amplitude shifts of said peaks.

Based on the reported literature review, it seems that vibroacoustic measurements carry relevant information about the AWJC process, which can be effectively used for monitoring its parameters, extracting performance and quality indicators, as well as diagnosing the health status of the head components. Furthermore, the measured quantities have proven to be related to the energy and forces delivered to the workpiece by the cutting head, hence the jet cutting capability. Indeed, contributions like [18][19] clearly show the possibility of monitoring the jet cutting capability by means of vibration sensors attached on the workpiece.

However, the previous setups have the drawback of being dependent upon the specific configuration of each workpiece. Indeed, the mounting and dismounting of the sensing devices would be constantly required once the workpiece is changed, with a negative impact on the robustness and reproducibility of the whole measurement process. Besides, the process downtimes would be negatively affected, as well. For such reason, an ideal monitoring setup that is limited to the components of the AWJC apparatus and does not extend to the workpiece is expected to be much more effective in a real production environment.

The present paper aims at filling the aforementioned gap by introducing an AWJC focusing tube instrumented with two accelerometers, which are exploited for monitoring its operational vibration. It is proven how the monitored data can be processed in real time, to deliver an innovative indicator of the jet cutting capability that involves the relevant effects of all the process parameters. With respect to the state of the art, the proposed monitoring method does not include sensors on the workpiece and this feature makes the setup more robust, as

well as fully compatible with day-to-day operations. By delivering a real-time indicator of the jet cutting capability, the instrumented focusing tube could represent a valuable tool for enabling innovative closed-loop control systems of p and m_a , thus tacking the requirements of power users for improved process tracking and stabilization. The present contribution is structured as follows: in Section 2, the theoretical jet power is introduced, which is used as a quantitative indicator of the jet cutting capability; the materials and methods are presented in Section 3; Section 4 describes the experimental campaign and discusses the results; Section 5 draws the conclusions of the work.

2 Theoretical background and jet power definition

In order to achieve an effective monitoring of the waterjet cutting performance, this paper defines the jet power P_{part} starting from the typical relationships existing among the waterjet quantities, which are taken from [3]. First, the waterjet theoretical velocity v_{th} , i.e. the velocity assumed by the waterjet in air after converting its pressure energy into kinetic energy, can be obtained from the Bernoulli equation (Eq. 1). The Bernoulli equation can be improved by considering the water compressibility, which plays a relevant role at the very high pressures of the waterjet cutting applications: the correspondent expression of the theoretical compressible velocity $v_{\text{th,c}}$ is stated in Eq. 2, where C and L are two constants. The coefficient ψ , which is the ratio between $v_{\text{th,c}}$ and v_{th} , captures the water compressibility, while the velocity coefficient c_v considers the energy losses due to the irreversible thermodynamic transformation of the water flowing through the orifice. These two coefficients allow calculating the real jet velocity v_j , i.e. the pure waterjet velocity in air, starting from v_{th} (Eq. 3). Subsequently, it is possible to obtain the water mass flow rate m_w from Eq. 4, where the water volume flow rate Q_w is computed as the product of v_j and the jet cross-sectional area at the *vena contracta* S_j (Eq. 5). The contraction coefficient c_c allows calculating S_j from S_0 , the latter being the nominal cross-sectional area of the orifice. The product of c_v , c_c and ψ gives the discharge coefficient c_d . If c_d is known from the datasheet of a certain orifice, Q_w can be calculated as the product of c_d , S_0 and v_{th} (Eq. 5). The abrasive loading ratio r_d is introduced to explain the energy transfer from the water to the abrasive particles, which starts in the mixing chamber and continues inside the focusing tube (Figure 1, Eq. 6). In fact, the momentum balance between the incoming water, the abrasive, the air (i.e. the abrasive carrier from the hopper to the mixing chamber) and the mixed jet, whose velocity is v_{abr} , is dependent upon r_d (Eq. 7). It should be noted that v_{abr} is the velocity of both the water and the abrasive particles once these are completely mixed at the exit of the focusing tube and under the hypothesis of no energy losses. Finally, it is possible to express P_{part} as the only portion of the jet kinetic power that is useful for the material removal process, which means the kinetic power of the abrasive particles (Eq. 8). The jet power P_{part} will be used in the following part of this study, as a quantitative indicator of the jet cutting capability. Moreover, this paper will demonstrate how this indicator can be properly assessed by means of vibroacoustic acquisitions.

$$v_{\text{th}} = \sqrt{\frac{2p_0}{\rho_1}} \quad \text{Eq. 1}$$

$$v_{\text{th,c}} = \sqrt{\frac{2L}{\rho_1(1-C)} \left[\left(1 + \frac{p_0}{L}\right)^{1-C} - 1 \right]} \quad \text{Eq. 2}$$

$$v_j = c_v v_{\text{th,c}} = c_v \psi \sqrt{\frac{2p_0}{\rho_1}} \quad \text{Eq. 3}$$

$$m_w = \rho_1 Q_w \quad \text{Eq. 4}$$

$$Q_w = S_j v_j = c_c S_0 v_j = c_c \frac{d_n^2 \pi}{4} c_v \psi \sqrt{\frac{2p_0}{\rho_1}} = c_d \frac{d_n^2 \pi}{4} \sqrt{\frac{2p_0}{\rho_1}} \quad \text{Eq. 5}$$

$$r_d = \frac{m_a}{m_w} \quad \text{Eq. 6}$$

$$v_{\text{abr}} = \frac{v_j}{1 + r_d} \quad \text{Eq. 7}$$

$$P_{\text{part}} = \frac{1}{2} m_a v_{\text{abr}}^2 \quad \text{Eq. 8}$$

3 Materials and methods

3.1 AWJC system and instrumented focusing tube

The AWJC system used in the present investigation is an Intermac Primus 322 Metal installed at the Department of Mechanical Engineering of Politecnico di Milano (Italy). Its technical details are reported in Table 1. An estimation of the jet power attainable with this equipment has been computed by equations 1 through 8 and the result can be appreciated in Figure 4 and Figure 5. These graphs show the trends of P_{part} vs p (p is used in the following instead of p_0 for the sake of simplicity) and P_{part} vs m_a for their respective operating ranges. The obtained curves appear almost linear; as p or m_a reduces to zero, P_{part} reduces to zero as well. A variation of m_a affects the slope of the curve P_{part} vs p . A variation of p has an analogous effect on P_{part} vs m_a . The maximum esteemed P_{part} is about 1.9 kW and is obtained at p and m_a equal to 380 MPa and 350 g/min, respectively.


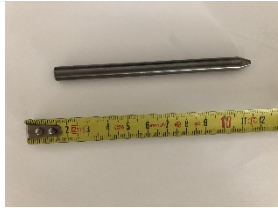
Pressure intensifier	Power:	37 kW	
	Max pressure:	380 MPa	
	Max flow rate:	3.5 l/min	
Handling system	5-axis cutting head		
	Longitudinal stroke X:	3210 mm	
	Transversal stroke Y:	2000 mm	
	Vertical stroke Z:	200 mm	
Cutting head	Primary orifice d_n :	0.33 mm	
	Focusing tube d_{awj} :	1.02 mm	
Focusing tubes	CERATIZIT Premium Line		
	d_{awj} :	1.02 mm	
	Outer \varnothing :	7.14 mm	
	Material:	Tungsten carbide	
	Length:	101.0 mm	
	Mass:	60.3 g	

Table 1. AWJC equipment and focusing tube.

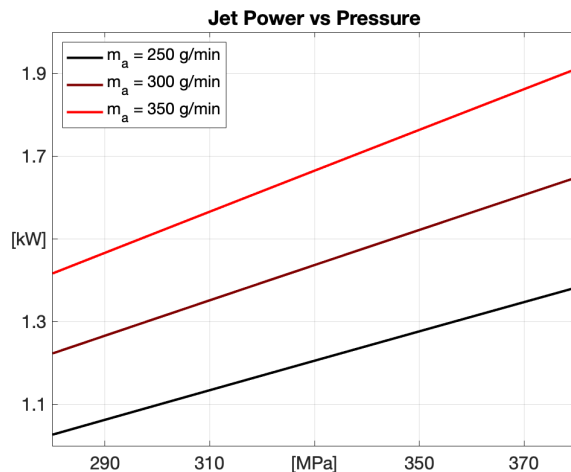


Figure 4. P_{part} vs p ($c_v=1$; $c_d=1$; water incompressibility).

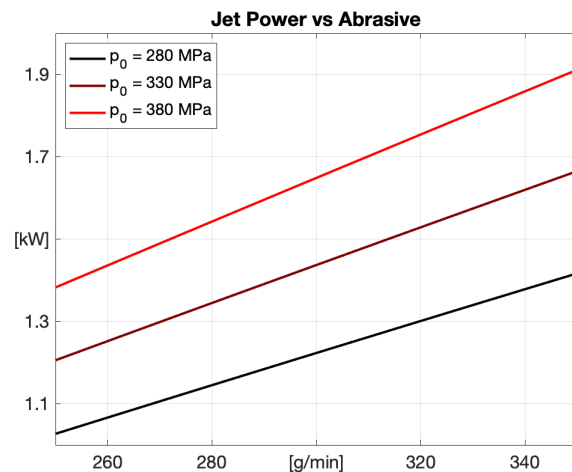


Figure 5. P_{part} vs m_a ($c_v=1$; $c_d=1$; water incompressibility).

The method presented in this paper is intended to extract an indicator of P_{part} from the operational vibration measured at the tip of the focusing tube. A 101.0 mm focusing tube (CERATIZIT Premium Line design) has been instrumented with two accelerometers (PCB 352C34 – ICP ceramic), whose technical specifications are reported in Table 2. The instrumented focusing tube is shown in Figure 6 and here the following components and features are visible: a steel adaptor with orthogonal side faces and an inner 7.2 mm hole; 10-32 screw holes on the side faces of the adaptor; the same adaptor, which is glued to the main body of the focusing tube by means of LOCTITE 648. Figure 7 shows the instrumented focusing tube installed, with the two accelerometers attached to the side faces of the adaptor, by means of 10-32 screw connections. The two accelerometers are indicated with the “downstream” labels: these lie on an orthogonal plane with respect to the axis of the focusing tube and are oriented

at 90 degrees, one respect to the other. The cable connectors are protected from the backscattered water with a silicon layer. The metallic plate, which has been initially included to prevent damaging of the sensing devices, has been subsequently removed. A third upstream accelerometer can also be noted (PCB 352C34 – ICP ceramic), which is attached to the clamp of the focusing tube by means of a magnet. The upstream accelerometer does not contribute to the method described hereafter, but it will help interpreting the results.

Sensitivity	99.6 mV/g at 100 Hz
Freq. response	10 to 10000 Hz
Resonance	60 kHz

Table 2. Technical specifications of the used accelerometers.

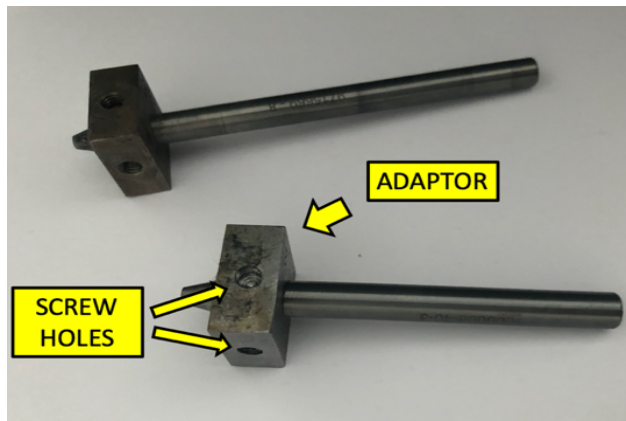


Figure 6. Instrumented focusing tubes.

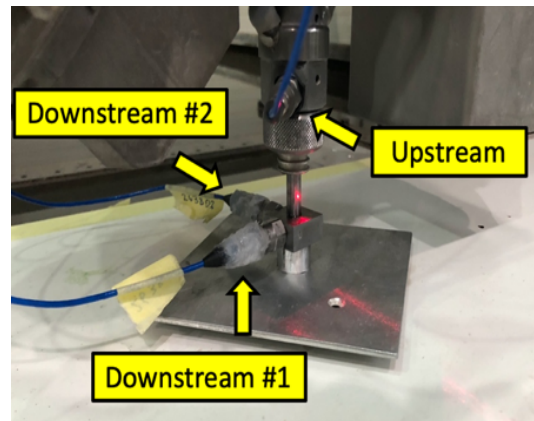


Figure 7. Accelerometers onboard.

3.2 Data processing method

The jet power P_{part} is the physical quantity that better represents the jet cutting capability. Hence, it would be extremely important to monitor and control this quantity during cutting operations. The following method is proposed for extracting an indicator of P_{part} from the operational vibration delivered by the instrumented focusing tube, which is hereafter referred to as power index:

1. Once the AWJC machine has been started, the operational vibration is monitored by means of the two accelerometers of the focusing tube. The signals acquisition is carried out by means of a National Instruments CDAQ 9232 Sound & Vibration module, at a sampling frequency of 102.4 kHz and a recording period of 15 s. The acquisition trigger is set on one of the two channels, indistinctly, at a level of 0.981 m/s^2 . A pre-trigger of 1 s is used. The correspondent time signals can be appreciated in Figure 8.
2. Transient vibration phenomena occur within the first 5 s after cutting process start-up. The transient period is truncated from each time signal, leaving only the steady portion of 10 s for the next processing steps.
3. For each signal, the Welch's method [24] is adopted for computing the corresponding Power Spectral Density (PSD) on the remaining 10 s signal chunk (100 averages, no overlap, hamming window). The PSDs of the two signals are shown in Figure 9 (here it is also reported the PSD of the upstream signal, for next considerations).
4. Subsequently, the two PSDs are summed into a total PSD. Finally, the integral of the total PSD is computed in a predetermined frequency interval. Said integral constitutes the power index and it is shown in Figure 10 for two intervals, namely 500 Hz to 10 kHz and 10 kHz to 50 kHz, which will be hereafter referred to as the low range and the high range, respectively. The first corresponds to the operational range of the accelerometers, minus the range 10-500 Hz as the latter does not carry information highly related to the investigated phenomena. The high range reaches up to the Nyquist frequency of the acquisition module and here the accelerometers operate out of their specifications, hence a signal distortion should be expected. Moreover, as reported in [22], it is expected that water contributes more in the low frequency range, while abrasive particles provide their vibration signature above 10 kHz. This further justifies the choice of 10 kHz as threshold between the two investigation ranges.

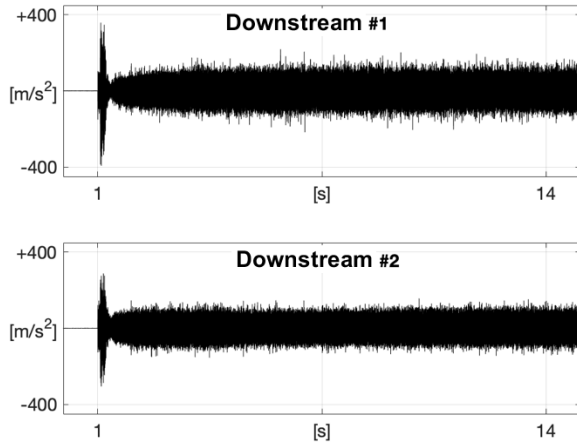


Figure 8. Time signals ($p = 330$ MPa; $m_a = 300$ g/min).

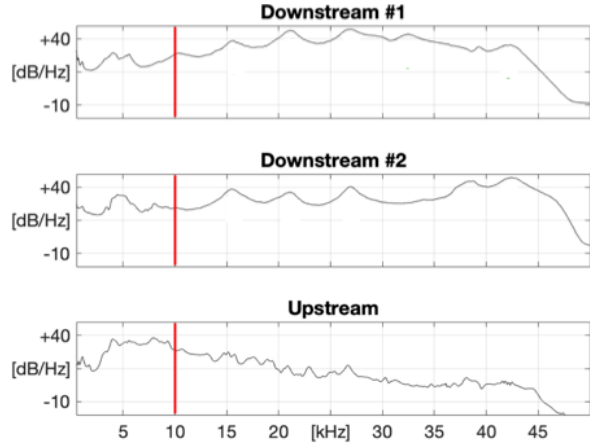


Figure 9. PSDs ($p = 330$ MPa; $m_a = 300$ g/min). dB reference: $1e-6$ m/s².

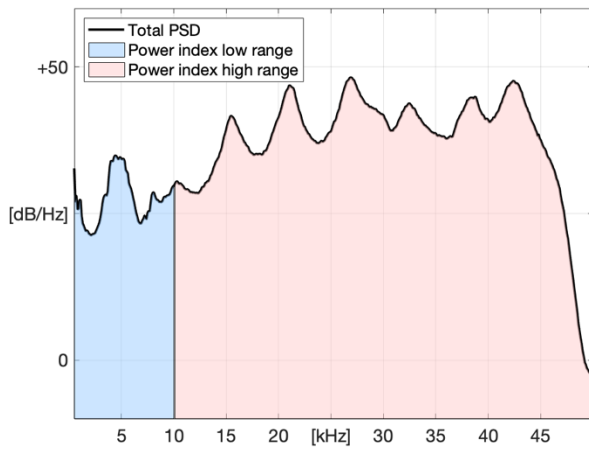


Figure 10. Total PSD and power indices ($p = 330$ MPa, $m_a = 300$ g/min). dB reference: $1e-6$ m/s².

4 Results and discussion

The experimental campaign has been carried out by using a Barton Garnet, Mesh-80 abrasive. Here, p and m_a have been selected as the controlled parameters of the AWJC process. A full-factorial test design has been developed, consisting of the nine combinations (set points) of p and m_a reported in Table 3 and ten replications per set point, providing a total number of ninety tests for the experimental campaign. For each test, the set point has been chosen randomly among those of Table 3 and subsequently the waterjet fired for 15 s, without workpiece and the head maintained in steady position.

	280 MPa	330 MPa	380 MPa
250 g/min	LP-LA	MP-LA	HP-LA
300 g/min	LP-MA	MP-MA	HP-MA
350 g/min	LP-HA	MP-HA	HP-HA

Table 3. Setpoints.

During each test, the operational vibration has been monitored and processed according to the method detailed previously. As said, this monitoring and processing strategy is based on the generated vibration as a means to collect information about the jet power: in a way, the present method resembles those previously mentioned among the state-of-the-art (in particular [18][19]); however, the differences among the setups (in particular the absence of analogous measurements of the focusing tube operational vibration) prevent comparisons with prior data. Two frequency intervals have been considered for the computation of the power index, namely the low range and the high range (Section 3.2). Figure 11 and Figure 12 show the total PSDs gathered during the 90 tests, for the low range and the high range, respectively. An outlier analysis of the correspondent power indices has been carried out and it is shown in Figure 13 and Figure 14: here, all the experimental points fall within a confidence interval of 95 % except two, which are slightly outside but have been maintained, nevertheless.

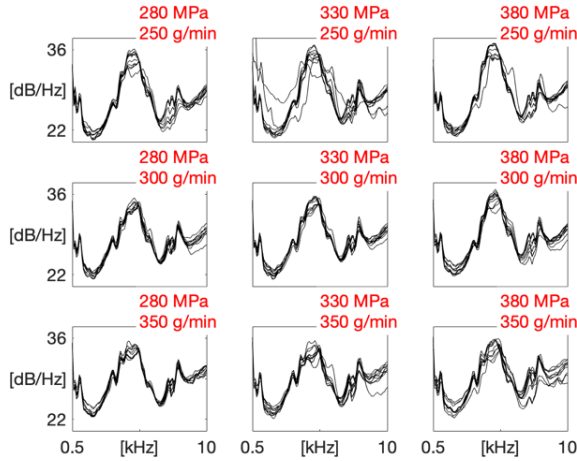


Figure 11. Total PSDs for all the tests (low range). dB reference: $1e-6 \text{ m/s}^2$.

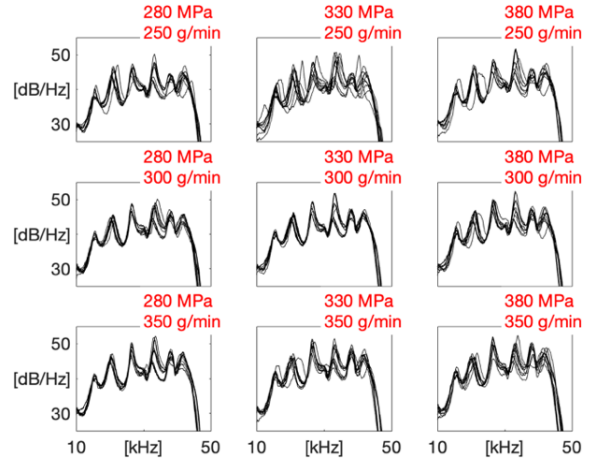


Figure 12. Total PSDs for all the tests (high range). dB reference: $1e-6 \text{ m/s}^2$.

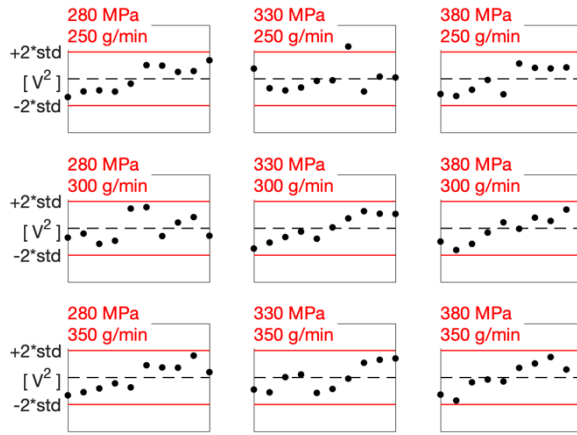


Figure 13. Outlier analysis of the power indices (low range).

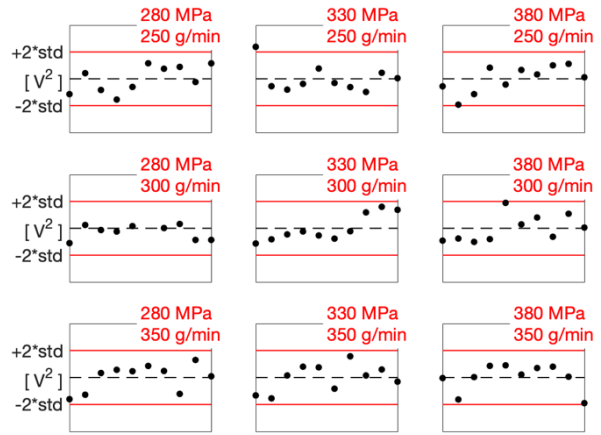


Figure 14. Outlier analysis of the power indices (high range).

Figure 15 compares the power indices, which are computed on the low range: here, each black dot corresponds to the power index of one replication; each red dot is the arithmetic average of the ten replications of the correspondent set point; the left column shows a comparison of tests at different p , i.e. the rows of Table 3; on the right column, the comparison is carried out for tests at different m_a , i.e. the columns of Table 3; the green lines are the theoretical trends expected, according to equations 1 through 8; a calibration factor of $1.68e8 \text{ W}/(\text{V}^2/\text{Hz})$ has been used for multiplying the power indices. Analogous comparisons are shown Figure 16, but here the power indices are computed on the high range and the correspondent calibration factor is $2.28e6 \text{ W}/(\text{V}^2/\text{Hz})$. Both the calibration factors have been computed using a least squares criterion, more specifically: the relative square errors have been computed between the nine arithmetic averages (red dots), multiplied by the unknown calibration factor, and the correspondent theoretical values (green line); subsequently, the relative square errors have been summed into a total error and the calibration factor has been set to the value that minimizes the latter. The low range and the high range show different calibration factors, which is considered a legitimate consequence of the Frequency Response Functions (FRFs) of both the sensors and the AWJC apparatus. The relative square errors between the calibrated red dots and the respective theoretical values are reported in Table 4 and Table 5 for the low range and the high range, respectively. An analysis of variance (ANOVA) has been applied to the data set, which has showed that the effects of p and m_a on the power index are statistically significant, for both the low range and the high range. However:

- The PSDs in the low range and consequently the correspondent power indices show a relevant dispersion within the replications of the same set point; this is particularly evident for the pressure comparisons at low and high abrasive, as well as the abrasive comparisons at middle and high pressure. Furthermore, the outlier of Figure 13 diverges significantly from the theoretical value expected. On the other hand, the dispersion of the experimental data within the replications of the same set point is lower in the high range.
- For both the low range and the high range, the maximum standard deviations of the experimental data points occur at the MP-LA set point and equal 0.21 and 0.12 kW, respectively. Hence, the minimum jet power

fluctuations that are detectable within a confidence interval of 68 % are 0.42 kW (low range) and 0.24 kW (high range).

- In the high range, the power indices increase with both the abrasive mass flow rate and the water pressure, showing a substantial agreement with the theoretical jet power. In the low range, the power indices do not fit well the theoretical trend; this is particularly evident in the pressure comparisons at low and high abrasive, as well as the abrasive comparison at high pressure. Consequently, the relative square errors in the low range are substantially higher, with respect to the high range.

	280 MPa	330 MPa	380 MPa
250 g/min	15.8 %	19.5 %	10.7 %
300 g/min	1.9 %	5.8 %	8.6 %
350 g/min	3.5 %	11.5 %	14.1 %

Table 4. Relative square errors (low range). Average = 10.2 %.

	280 MPa	330 MPa	380 MPa
250 g/min	3.7 %	6.0 %	4.5 %
300 g/min	1.8 %	0.9 %	3.4 %
350 g/min	11.0 %	4.8 %	3.2 %

Table 5. Relative square errors (high range). Average = 4.4 %.

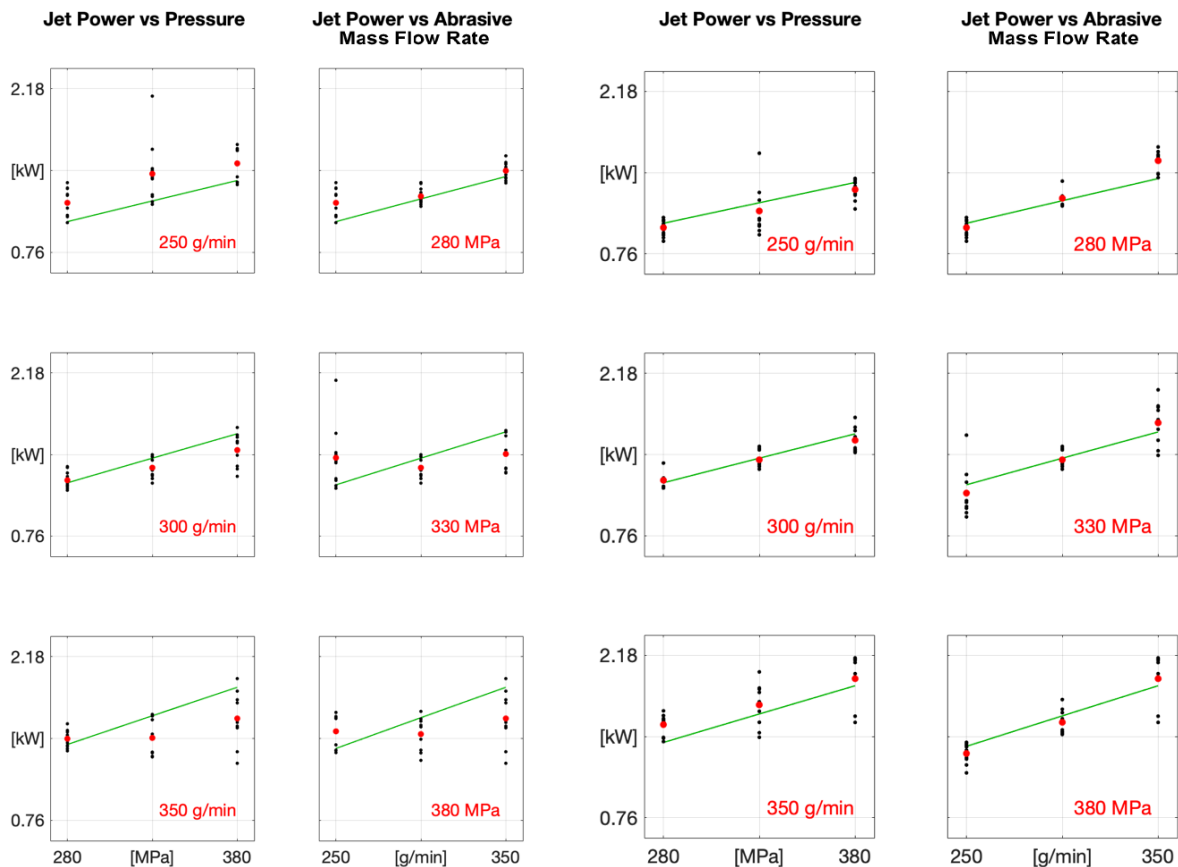


Figure 15. Comparison (low range). Green lines: theoretical trends. Black dots: power indices. Red dots: arithmetic averages.

Figure 16. Comparison (high range). Green lines: theoretical trends. Black dots: power indices. Red dots: arithmetic averages.

According to the results, the power index computed in the high range provides a more robust and accurate indicator of the jet power, with respect to the one computed in the low range. A further consideration can be made, regarding the vibration levels. Indeed, the PSDs in the high range exceed those in the low range of about 15 dB, which is quite singular, given the frequencies involved. In conclusion, two questions are left open for the

interpretation of the results i.e. the higher vibration levels in the high range and the better performance of the power index in the high range.

The following part of this section provides an explanation to the higher vibration level in the high range, with respect to the low range. Further, the physical relation between the jet power and the generated vibration, hence the power index, is investigated. Considerations are also made, for explaining the better performance of the power index in the high range.

4.1 Analysis of the vibration levels

A typical drawback of accelerometers, for many applications, is the amplification effect that is produced at high frequencies. Such distortion should always be considered and characterized, especially when the sensor is intended to be operated for quantitative assessments of the vibration response of a system. To characterize the distortion effect introduced by the accelerometers when monitoring vibration phenomena outside their working range, a dedicated test was performed aimed at comparing the vibration signals recorded by the accelerometer and a Laser Doppler Vibrometer (LDV).

The AWJC apparatus has been operated at p and m_a equal to 380 MPa and 350 g/min, respectively. The operational vibration has been measured by means of one accelerometer of the focusing tube. At the same time, a non-contact measurement has been carried out by means of a single-point LDV, as shown in Figure 17: it can be noticed the LDV spot nearby the location of the accelerometer, as well as the orientation of the laser, which is aligned with the sensing direction of the same accelerometer. Figure 18 shows the PSDs measured by the LDV and the accelerometer, with the latter that is integrated into velocity, to obtain comparable data sets. Such comparison is intended to enhance the different performance between the two sensors, in terms of sensitivity: in the low range, no relevant frequency or amplitude discrepancies can be noticed between the two data sets; instead, in the high range the accelerometer amplifies certain vibration phenomena more than the LDV because the former is working outside its standard working range.

It is evident that, for the present application, the signal distortion introduced by the accelerometer in the high range could be interpreted as a positive side effect, since it highlights the portion of vibration energy that correlates better with the jet power.

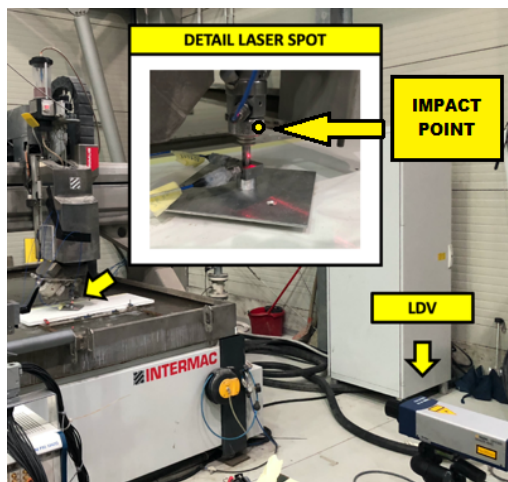


Figure 17. Experimental LDV setup. LDV sensitivity: 100 mV/mm/s.

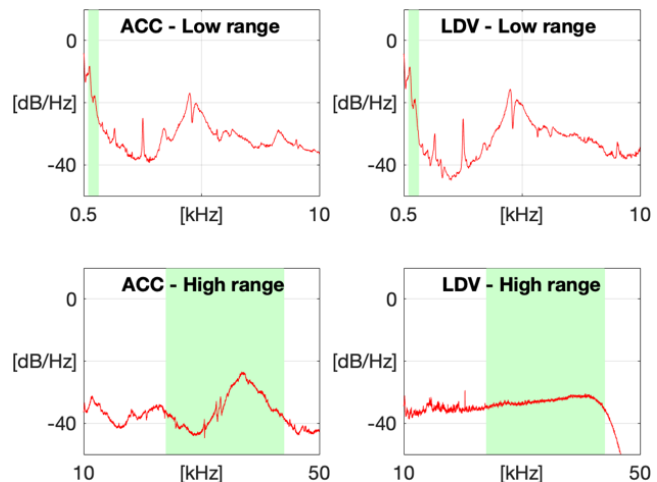


Figure 18. PSDs (accelerometer and LDV). Accelerometer integrated into velocity. dB reference: $1e-9$ m/s.

4.2 Physical relation between the jet power and the generated vibration

During operation, abrasive particles travel through the focusing tube and produce shallow impacts with its inner surface. Said impacts constitute a relevant mechanical phenomenon for the focusing tube, which results in a regime temperature of about 70 °C, fast wear progression and a service life down to 100 hours. The method described in this paper grounds on the fundamental hypothesis that impacts produced by the abrasive particles generate a random excitation whose cut-off frequency is well above the sampling frequency adopted in the monitoring operations. The focusing tube responds to this random excitation by vibrating at its resonance frequencies. The main hypothesis done here is that a variation in the kinetic energy and flow rate of the particles, hence in the jet power, should be highly correlated to the vibration response of the focusing tube if this response is observed in terms of its energy change (e.g. modification of the amplitude of the PSD associated to the vibration

signal) rather than in terms of frequency changes (as it may happen if a change in the focusing tube takes place – e.g. increase of its inner diameter due to wear phenomena).

Following such hypothesis, the factor that is expected to discriminate between the low range and the high range, in terms of performance of the power index, are the types of modes involved. In particular, the vibration energy in the low range is expected to be associated with global modes of the focusing tube and the whole cutting head. Said modes are affected by the instantaneous configuration of the cutting head itself and secondary phenomena with respect to the jet power. Moreover, likely non-linear dynamic behaviour of the cutting head (due to the mechanical connections of the whole assembly) could be involved in the low-frequency range that might also affect the response to variations of the jet power. On the other hand, the vibration energy in the high range is expected to be associated with local modes of the focusing tube, which are less influenced by further variables, besides the jet power.

To support this conclusion, a combined numerical-experimental investigation has been conducted, for characterizing the focusing tube dynamics and identifying its global vibration modes. A Finite Element (FE) model of the focusing tube has been developed with MATLAB®, using a one-dimensional mesh along its axis. The geometrical features of the cross section are those reported in Table 1. The Young modulus and mass density have been set to 620 GPa and 15700 kg/m³, respectively, according to the material data provided by the manufacturer. A lumped mass of 43.3 grams has been located at the correspondent position of the steel adaptor, which is 10 mm from the tip, and it equals the total mass of the adaptor itself and the two accelerometers. The clamp has been approximated as a perfect lock of both the translational and rotational degrees of freedom. Figure 19 shows the simulations of the first three bending modes, with their respective natural frequencies. At the same time, an instrumented focusing tube has been installed on the AWC system and its tip vibration has been measured by means of an LDV, during an impact test. Here six strikes have been carried out, by means of an impact hammer (model Brüel & Kjær type 8204, sensitivity 22.7 mV/N), with an average impact peak magnitude of 0.1 N. The impact point (also referred to as driving point) was chosen on the focusing tube itself and nearby the clamp with the cutting head, as indicated in Figure 17. Figure 20 shows the computed Frequency Response Function (FRF), which has been averaged over the results of the six tests: it can be noted an amplification at about 970 Hz, which is highlighted in green and dominates the total response. Said amplification matches the numerical prediction of the first natural frequency of the focusing tube and the agreement can be taken as a validation of the numerical model.

Therefore, the same numerical model can be exploited for extrapolating with reasonable confidence the other two natural frequencies, i.e. 18 and 55 kHz, hence proving that the high range is substantially free of global vibration modes. One last consideration can be made by looking at Figure 9, which compares the PSD upstream with the two downstream: in the low range, the upstream level is comparable with the two downstream, suggesting that the correspondent vibration is global and involves the whole apparatus; on the other hand, in the high range the upstream level drops of about 30 dB, suggesting that the correspondent vibration is local and limited only to the focusing tube.

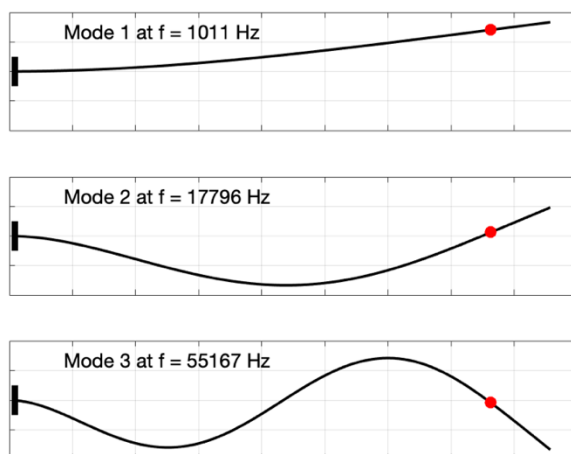


Figure 19. Numerical bending modes of the focusing tube. The constraint is on the left side. The red dot represents the lumped mass.

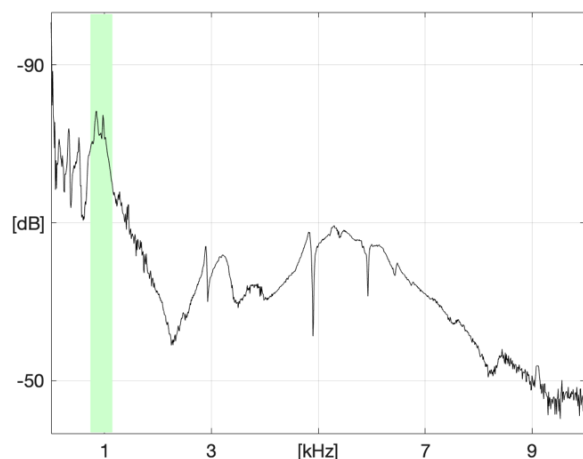


Figure 20. Frequency Response Function of the focusing tube. dB reference: 1 g/N.

In conclusion, the power index computed in the high range is well related to the impacts of the abrasive particles against the inner wall of the focusing tube, therefore to the jet power. On the other hand, the power index computed in the low range is related to the global modes of the focusing tube and the whole AWJC apparatus, so it should be less significant for the purpose of jet power monitoring. According to these considerations, the power index

computed in the high range correctly represents the jet power, therefore can be used for monitoring purposes: variations of p and m_a produce a variation of the jet power and consequently of the power index. At the same time, when a monitoring function detects a fluctuation of the power index, control actions can be made on p and m_a for compensating and maintaining the jet power at the benchmark value.

The approach presented in this paper is successful in enabling a continuous monitoring, tracking and control of the abrasive waterjet cutting capability. As a last note, it should be considered that the present investigation has been carried out with the cutting head in a steady position: indeed, its movement was found to negatively affect the performance of the method. Given that and following the indications from industrial partners, it can be imagined a new “calibration stage”, in which the waterjet is fired at steady head and before attacking the workpiece; once the power index is delivered, p and m_a can be retro-controlled, in order to bring the jet power at the benchmark level; subsequently, the machining operation can start. The development of such an exploitation procedure for the new “smart” focusing tube will be the object of a follow-up activity.

5 Conclusions

A focusing tube for abrasive waterjet cutting has been presented, which is instrumented with two accelerometers for monitoring the operational vibration. Tests have been carried out at different water pressures and abrasive mass flow rates, providing different jet powers, as indicated by the governing equations of the abrasive waterjet process physics. The operational vibration has been processed, to extract an indicator called power index. It has been demonstrated that said indicator correlates linearly with the jet power, i.e. the jet cutting capability, which is a new and valuable result for abrasive waterjet monitoring and controlling purposes. Consequently, the operational vibration can effectively be exploited as the monitored variable for closing the control loops of the water pump and the abrasive feeder, thus improving the process stability, as well as allowing the process tracking. With respect to the previous state of the art, the present approach does not entail the presence of sensors on the workpiece. This feature is expected to make the setup more robust and compatible with day-to-day operations of a real production environment.

Funding

This work was supported by the project SHIM. The project receives funding under the JUMP Program of the Luxembourg National Research Fund (FNR), grant agreement n. PoC19/13599764/SHIM.

Notes and acknowledgements

The authors would like to kindly acknowledge CERATIZIT Luxembourg S.à r.l. and FLOW INTERNATIONAL CORPORATION for the fruitful discussions during the activity.

The authors would like to kindly acknowledge CERATIZIT Luxembourg S.à r.l. for having supported the SHIM project by providing specimens and consumables.

The systems and methods for monitoring the operational vibration and delivering the power index from the signals are the objects of two patent applications [25][26]. The intellectual property included in said patents belongs to the University of Luxembourg.

The Department of Mechanical Engineering of Politecnico di Milano provided the knowledge about the AWJC process and its physical description at the base of the theoretical definition of the jet power.

The Department of Industrial Engineering and Mathematical Sciences of Università Politecnica delle Marche contributed to the performance validation of the instrumented focusing tube by developing and deploying the non-contact measurement setups.

References

- [1]. H. T. Liu, “Waterjet technology for machining fine features pertaining to micromachining”, *Journal of Manufacturing Processes*, vol.12 (1), pp. 8-18, 2010. DOI: <https://doi.org/10.1016/j.jmapro.2010.01.002>.
- [2]. A. Rabani, J. Madariaga, C. Bouvier, D. Axinte, “An approach for using iterative learning for controlling the jet penetration depth in abrasive waterjet milling”, *Journal of Manufacturing Processes*, vol. 22, pp. 99-107, 2016. DOI: <http://dx.doi.org/10.1016/j.jmapro.2016.01.014>.
- [3]. M. Hashish, “Pressure effects in abrasive waterjet (AWJ) machining, *Journal of Engineering Materials and Technology*”, *Transactions of the ASME*, vol. 111, issue 3, pp. 221-228, July 1989. DOI: <https://doi.org/10.1115/1.3226458>.
- [4]. M. Annoni, F. Arleo, F. Viganò, 2017, *Micro-waterjet Technology*. In: Fassi I., Shipley D. (eds) *Micro-Manufacturing Technologies and Their Applications*. Springer Tracts in Mechanical Engineering, pp. 129-148.

- [5]. A. W. Momber, R. Kovacevic, "Principles of abrasive water jet machining", Springer Science & Business Media, 2012. DOI: <https://doi.org/10.1007/978-1-4471-1572-4>.
- [6]. M. Hashish, "Observations of wear of abrasive-waterjet nozzle materials", *Journal of Tribology*, vol. 116, issue 3, pp. 439-444, 1994. DOI: <https://doi.org/10.1115/1.2928861>.
- [7]. K. Kalpana, O. V. Mythreyi, M. Kanthababu, "Review on condition monitoring of Abrasive Water Jet Machining system", *Proceedings of the 2015 International Conference on Robotics, Automation, Control and Embedded Systems (RACE)*, 2015. DOI: 10.1109/RACE.2015.7097254.
- [8]. A. I. Hassan, C. Chen, R. Kovacevic, "On-line monitoring of depth of cut in AWJ cutting", *International Journal of Machine Tools and Manufacture*, vol. 44, issue 6, pp. 595-605, 2004. DOI: <https://doi.org/10.1016/j.ijmachtools.2003.12.002>.
- [9]. B. Jurisevic, D. Brissaud, M. Junkar, "Monitoring of abrasive water jet (AWJ) cutting using sound detection", *The International Journal of Advanced Manufacturing Technology*, vol. 24 (9-10), pp. 733-737, 2004. DOI: <https://doi.org/10.1007/s00170-003-1752-5>.
- [10]. J. Valíček, S. Hloch, "Using the acoustic sound pressure level for quality prediction of surfaces created by abrasive waterjet", *The International Journal of Advanced Manufacturing Technology*, vol. 48 (1-4), pp. 193-203, 2010. DOI: <https://doi.org/10.1007/s00170-009-2277-3>.
- [11]. V. Peržel, P. Hreha, S. Hloch, H. Tozan, J. Valíček, "Vibration emission as a potential source of information for abrasive waterjet quality process control", *The International Journal of Advanced Manufacturing Technology*, vol. 61 (1-4), pp. 285-294, 2012. DOI: <https://doi.org/10.1007/s00170-011-3715-6>.
- [12]. P. Hreha, A. Radvanská, S. Hloch, V. Peržel, G. Królczyk, K. Monková, "Determination of vibration frequency depending on abrasive mass flow rate during abrasive water jet cutting", *The International Journal of Advanced Manufacturing Technology*, vol. 77 (1-4), pp. 763-774, 2015. DOI: <https://doi.org/10.1007/s00170-014-6497-9>.
- [13]. I. A. Popan, V. Bocanet, N. Balc, A. I. Popan, "Investigation on feed rate influence on surface quality in abrasive waterjet cutting of composite materials", *Proceedings of the International Conference on Advances in Manufacturing Engineering and Materials*, pp. 105-113, 18-22 June 2018, Nový Smokovec, Slovakia. DOI: https://doi.org/10.1007/978-3-319-99353-9_12.
- [14]. R. Pahuja, M. Ramulu, Abrasive waterjet process monitoring through acoustic and vibration signals, *Proceeding of the 24th Conference on Water Jetting*, 5-7 September 2018, Manchester, UK. ISBN: 978-1-5108-7523-4.
- [15]. P. Sutowski, M. Sutowska, W. Kaplonek, The use of high-frequency acoustic emission analysis for in-process assessment of the surface quality of aluminium alloy 5251 in abrasive waterjet machining, *Proceedings of the Institution of Mechanical Engineers, Part B: Journal of Engineering Manufacture*, vol. 232 (14), pp. 2547-2565, 2018. DOI: <https://doi.org/10.1177/0954405417703428>.
- [16]. R. Pahuja, M. Ramulu, Surface quality monitoring in abrasive water jet machining of Ti6Al4V-CFRP stacks through wavelet packet analysis of acoustic emission signals, *The International Journal of Advanced Manufacturing Technology*, vol. 104 (9-12), pp. 4091-4104, 2019. DOI: <https://doi.org/10.1007/s00170-019-04177-0>.
- [17]. L. Huaizhong, Monitoring the abrasive waterjet drilling of Inconel 718 and steel: a comparative study, *The International Journal of Advanced Manufacturing Technology*, vol. 107, pp. 3401-3414, 2020. DOI: <https://doi.org/10.1007/s00170-020-05246-5>.
- [18]. D. A. Axinte, M. C. Kong, "An integrated monitoring method to supervise waterjet machining", *CIRP annals*, vol. 58 (1), pp. 303-306, 2009. DOI: <https://doi.org/10.1016/j.cirp.2009.03.022>.
- [19]. A. Rabani, I. Marinescu, D. Axinte, "Acoustic emission energy transfer rate: A method for monitoring abrasive waterjet milling", *International journal of machine tools and Manufacture*, vol. 61, pp. 80-89, 2012. DOI: <https://doi.org/10.1016/j.ijmachtools.2012.05.012>.
- [20]. R. Kovacevic, M. Evizi, "Nozzle wear detection in abrasive waterjet cutting systems", *Materials Evaluation*, vol. 48 (3), pp. 348-353, 1990.
- [21]. R. Kovacevic, L. Wang, Y. M. Zjang, "Detection of Abrasive Waterjet Nozzle Wear Using Acoustic Signature", *Proceedings of the American Waterjet Conference*, vol. 7, pp. 217-232, 1993.

- [22]. R. Kovacevic, L. Wang, Y. M. Zhang, "Identification of abrasive waterjet nozzle wear based on parametric spectrum estimation of acoustic signal", Proceedings of the Institution of Mechanical Engineers, Part B: Journal of Engineering Manufacture, vol. 208 (3), pp. 173-181, 1994. DOI: https://doi.org/10.1243/PIME_PROC_1994_208_076_02.
- [23]. P. Hreha, A. Radvanská, J. Cárach, D. Lehocká, K. Monková, G. Krolczyk, A. Ruggiero, I. Samardzić, D. Kozak, S. Hloch, "Monitoring of focusing tube wear during abrasive waterjet (AWJ) cutting of AISI 309", Metalurgija, vol. 53 (4), pp. 533-536, 2014. ISSN: 0543-5846.
- [24]. P. D. Welch,, "The use of Fast Fourier Transform for the estimation of power spectra: A method based on time averaging over short, modified periodograms", IEEE Transactions on Audio and Electroacoustics, vol. 15 (2), pp. 70-73, 1967. DOI: 10.1109/TAU.1967.1161901
- [25]. E. Copertaro, "Abrasive waterjet cutting system, nozzle for such a system and monitoring process for such an abrasive waterjet cutting system", Publication No. WO 2020/064974 A1, International Application No. PCT/EP2019/076119, filed 26/10/2019, published 02/04/2020.
- [26]. E. Copertaro, "Machining system and monitoring method", Publication No. WO 2020/128090 A1, International Application No. PCT/EP2019/086911, filed 23/12/2019, published 25/06/2020.